

Provided for non-commercial research and education use.
Not for reproduction, distribution or commercial use.



This article appeared in a journal published by Elsevier. The attached copy is furnished to the author for internal non-commercial research and education use, including for instruction at the authors institution and sharing with colleagues.

Other uses, including reproduction and distribution, or selling or licensing copies, or posting to personal, institutional or third party websites are prohibited.

In most cases authors are permitted to post their version of the article (e.g. in Word or Tex form) to their personal website or institutional repository. Authors requiring further information regarding Elsevier's archiving and manuscript policies are encouraged to visit:

<http://www.elsevier.com/copyright>



Structural engineering of Ba_{0.5}Sr_{0.5}TiO₃ epitaxial films

Y.Q. Wang ^{a,*}, W.S. Liang ^a, W.J. Kong ^b, Peter K. Petrov ^c, Neil M. Alford ^c

^a The Cultivation Base for State Key Laboratory, Qingdao University, No. 308 Ningxia Road, Qingdao, 266071, PR China

^b College of Physical Science, Qingdao University, No. 308 Ningxia Road, Qingdao, 266071, PR China

^c Department of Materials, Imperial College London, Exhibition Road, London, SW7 2AZ, United Kingdom

ARTICLE INFO

Article history:

Received 14 June 2011

Received in revised form 21 April 2012

Accepted 26 April 2012

Available online 3 May 2012

Keywords:

Barium strontium titanate

High-resolution transmission electron microscopy

Defects

Electrical properties

Pulse laser deposition

ABSTRACT

Ba_{0.5}Sr_{0.5}TiO₃ single-layered and multilayered films were epitaxially grown on a (001) LaAlO₃ substrate using single target and dual target pulsed laser deposition, respectively. Compared to the single-layered films, the multilayered films exhibited broader phase transition and improved thermo-stability. The microstructure of these epitaxial films was investigated using high-resolution transmission electron microscopy in details. Misfit and threading dislocations were observed in the single-layered film, while the threading dislocations were dramatically decreased and no misfit dislocations were found in the multilayered film. It is suspected that the difference in dislocation densities is responsible for the different behaviors of the permittivity with temperature.

© 2012 Elsevier B.V. All rights reserved.

1. Introduction

Ferroelectric thin films including BaTiO₃ (BTO), SrTiO₃ (STO) and (Ba, Sr) TiO₃ (BSTO) have received great attention because of their potential applications for various functional devices [1,2]. In BSTO films, the observed temperature (T_c) for the phase transition from paraelectric cubic to ferroelectric tetragonal and the stability of different phases depends on the microstructure and strain of the films. More significantly the peak in the temperature dependence of the dielectric permittivity is broader than that observed in bulk BSTO [3,4]. A broad peak in the dielectric response is desirable as the performance of the devices becomes less sensitive to temperature variations. Thus it is imperative to engineer a temperature-stable structure using different techniques. Researchers [3,4] have prepared BTO/STO superlattice films in order to make their dielectric properties less temperature sensitive. However, no investigation has been found in the literature to compare the nature of defect structures in the BSTO single-layered and BTO/STO multilayered films, and to correlate their microstructure with the dielectric properties.

In this paper, Ba_{0.5}Sr_{0.5}TiO₃ single-layered and (BTO)₅/(STO)₅ multilayered films were epitaxially grown on a (001) LaAlO₃ substrate using single-target and dual-target pulsed laser deposition (PLD) technique, respectively. The microstructure, especially the defect structure, was correlated with their dielectric properties. Misfit and threading dislocations were observed in the single-layered

Ba_{0.5}Sr_{0.5}TiO₃ film, while threading dislocations were dramatically decreased and no misfit dislocations were found in the multilayered film. It is suspected that the difference in dislocation densities is responsible for the different behaviors of the permittivity with temperature.

2. Experimental details

1- μ m-thick single-layered and multilayered films were epitaxially grown on a (001) LaAlO₃ substrate using PLD technique. As shown in Fig. 1, a single-layered epitaxial film was prepared using a single target of Ba_{0.5}Sr_{0.5}TiO₃, while the multilayered film with a periodic superlattice structure of BTO and STO layers with same thickness (~2 nm) was obtained using two stoichiometric targets of BaTiO₃ and SrTiO₃. The Ba_{0.5}Sr_{0.5}TiO₃ target for the PLD system was made using a mixed oxide route [5], while ultra-pure (Alfa Aesar) powders were used for the preparation of the BTO and STO targets.

The thin films were grown by laser ablation (Neocera PLD system with a Lambda Physik KrF laser, $\lambda = 248$ nm) on a 5 × 5 mm² LaAlO₃ substrates. The substrates were secured by silver paste onto the stainless-steel resistive heater. The thin films were deposited from 20-mm-diameter stoichiometric targets of BaTiO₃, SrTiO₃ and Ba_{0.5}Sr_{0.5}TiO₃ in an oxygen pressure of 40 Pa. The distance between the target and the substrate was 50 mm. The substrate temperature was kept at 750 K, and controlled using a thermocouple embedded in the heater during the deposition. The energy density of the laser spot (2 × 10 mm²) was 2.5 J/cm². The film thickness was controlled by the number of pulses shot on the targets. From the sample thickness measured using a Dektak 11A, the film growth rate was

* Corresponding author. Tel./fax: +86 532 83780318.
E-mail address: yqwang@qdu.edu.cn (Y.Q. Wang).

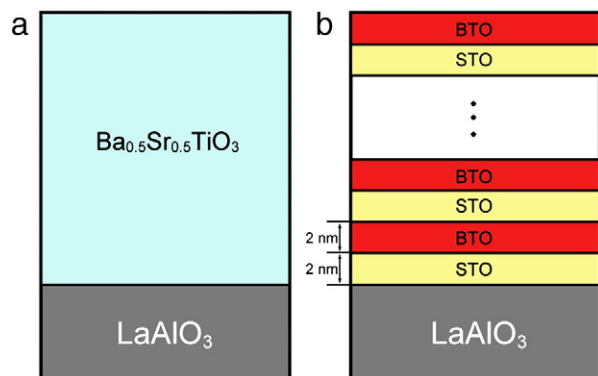


Fig. 1. (Color Online) Schematic diagram for the growth procedure of $\text{Ba}_{0.5}\text{Sr}_{0.5}\text{TiO}_3$ single layer (a) and BTO/STO superlattice (b).

estimated to be 0.05 nm/pulse. The total number of pulses was 5000 with a repetition rate of 8 Hz. Once the ablation was over, the samples were annealed for 1 h in an oxygen rich environment (1.01325×10^5 Pa) in order to reduce the oxygen vacancies, and then slowly cooled down to room temperature at a rate of $10^\circ\text{C}/\text{min}$.

The specimens for TEM examination were prepared in a cross-sectional orientation ([010] zone-axis for the LaAlO_3 substrate) using conventional techniques of mechanical polishing and ion thinning. The ion milling was performed using a Gatan Model 691 Precision Ion Polishing System. The bright-field (BF) imaging, selected-area electron diffraction (SAED) and HRTEM examinations were carried out using a JEOL JEM 2100F transmission electron microscope operating at 200 kV.

The electrical measurements of both single layered and multilayered films in a temperature range between 100 K and 400 K were performed on a Janis research cryogenic probe station. Agilent 4287A RF LCR meter was used for direct measurement of the capacitance and Q-factor of the samples.

3. Results and discussion

The single-layered film had capacitance vs. temperature dependence typical for a BSTO film with a Ba/Sr stoichiometry of 50/50, while the multilayered film had an almost linear dependence with an increment of ~ 0.1 pF/ $^\circ\text{C}$. Detailed electrical properties of the single-layered and multilayered films have been reported in Ref. [3]. It has been found that the multilayered film with the same stoichiometry exhibits broader phase transition and improved thermo-stability [3,4]. The temperature dependence is consistent with the previous study [6] of the BTO/STO superlattice grown on Nb-doped STO substrate. The multilayered films have reduced temperature dependence of capacitance, which indicates that it is much more promising for device applications. In order to give a comprehensive understanding of the differences in the electrical properties, we carried out a detailed investigation of the microstructure using conventional TEM and HRTEM.

Fig. 2(a) is a cross-sectional BF TEM image of the single-layered sample, while Fig. 2(b) is a cross-sectional BF TEM image of the multilayered sample. These diffraction contrast images were taken under a two-beam condition with $\mathbf{g} = 200$. Inset in Fig. 2(a) shows a typical [010] zone-axis SAED pattern taken from the single-layered film. The upper inset in Fig. 2(b) shows a typical [010] zone-axis SAED pattern taken from the superlattice, and the lower inset is an enlarged TEM image of the BTO/STO superlattice with a periodicity of 4 nm. Careful examinations of Fig. 2(a) and (b) show that there is a huge difference of the dislocation density. In Fig. 2(a), there are many dislocation lines, while in Fig. 2(b) some dislocations are suppressed in the region close to the interface between LaAlO_3 substrate and the multilayer stack, and very few dislocation lines

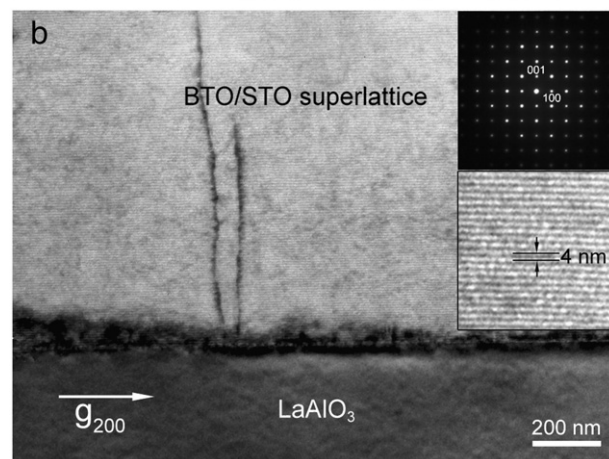
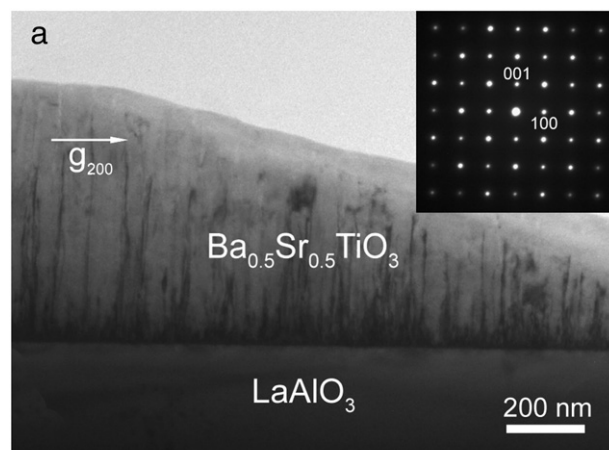


Fig. 2. (a) Cross-sectional BF image of $\text{Ba}_{0.5}\text{Sr}_{0.5}\text{TiO}_3/\text{LaAlO}_3$ taken near the [010] zone axis with a diffraction vector of $\mathbf{g} = 200$. Inset shows a typical [010] zone-axis SAED pattern taken from the epitaxial film. (b) Cross-sectional BF image of BTO/STO superlattice. Upper inset shows a typical [010] zone-axis SAED pattern taken from the superlattice region, lower inset is the enlarged TEM image of the BTO/STO superlattice.

penetrate through the whole film. This is consistent with the HRTEM observations of BTO/STO multilayered film with a periodicity of 3 nm [6]. The two images were taken under the same conditions, so the dislocation density reflects the true differences of microstructures for single-layered and multilayered films. The quality of the multilayered film is much better than that of the single-layered film. This is consistent with the report of BSTO film and artificial BTO/STO superlattices grown on Si substrates [7].

In order to clarify the nature of the defects, HRTEM was performed on both single-layered and multilayered films. Extensive HRTEM examinations showed that there are two kinds of dislocations in the single-layered sample while only one kind of dislocation exists in the multilayered film.

Fig. 3 shows an example of misfit and threading dislocations in the single layered sample. The misfit dislocation is shown in Fig. 3(a). Careful examination of Fig. 3(a) demonstrates that there is one extra half plane along the $[10\bar{1}]$ direction and another extra half plane along the $[101]$ direction near the interface regions, indicating that they belong to pure-edge type dislocations. The extra half planes are indicated by arrows for D1 and D2 in Fig. 3(a). To determine the Burgers vectors for the dislocations, Burgers circuits are drawn to enclose the dislocations. It can be clearly seen from Fig. 3(a) that there is a gap between the starting and ending point in each Burgers circuit, which is indicated by an arrow. The Burgers vector for dislocations D1 is determined to be $\frac{1}{2}[10\bar{1}]$. The Burgers vector for dislocations D2 is determined to be $\frac{1}{2}[101]$. Fig. 3(b) shows an

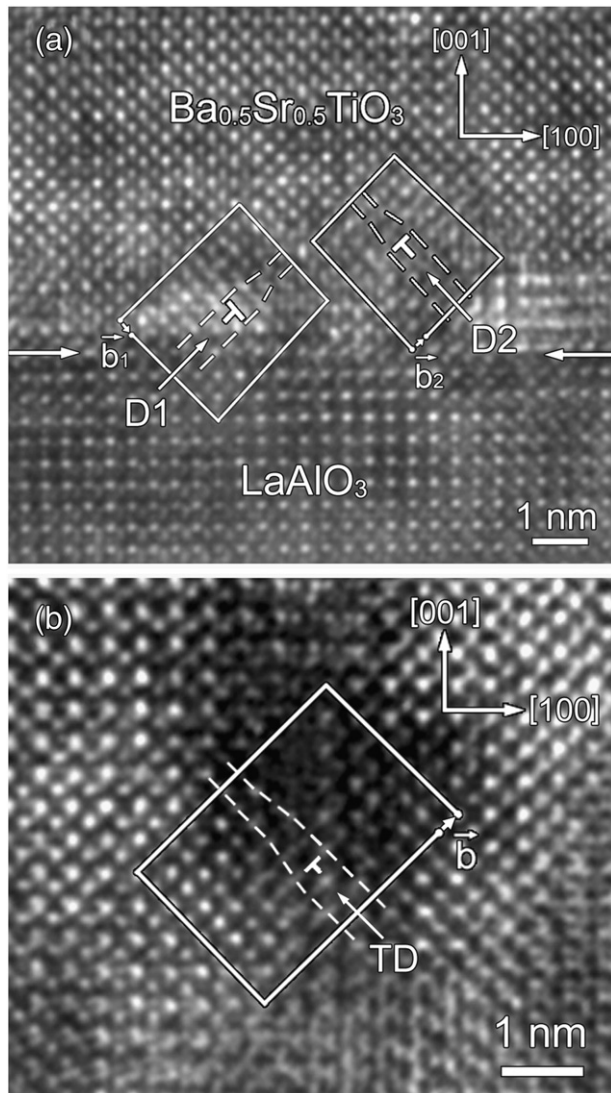


Fig. 3. HRTEM images of $\text{Ba}_{0.5}\text{Sr}_{0.5}\text{TiO}_3$ single-layered films showing different defect structures. (a) An example of misfit dislocations; (b) An example of a threading dislocation.

example of a threading dislocation. The Burgers vector for this threading dislocation is determined to be $\frac{1}{2} [101]$, which belongs to a partial dislocation. Similar dislocations have also been reported in the single-layered $\text{Ba}_{0.75}\text{Sr}_{0.25}\text{TiO}_3$ epitaxial films [8]. Apart from the dislocations, antiphase boundaries were also observed in the $\text{Ba}_{0.75}\text{Sr}_{0.25}\text{TiO}_3$ epitaxial film [9]. However, they have not been observed in the $\text{Ba}_{0.5}\text{Sr}_{0.5}\text{TiO}_3$ epitaxial film.

Fig. 4 shows an HRTEM image of a perfect region in the multilayered film. It can be clearly seen from Fig. 4 that there is no misfit dislocation in the multilayered film. The darker regions are BTO layers, while the brighter ones are STO layers. The thickness of each layer is about 2 nm, which corresponds to a stacking of 5-layered BTO and 5-layered STO. The lattice parameters of the BTO and STO layers were measured by a quantitative analysis of the HRTEM images using Gatan DIGITALMICROGRAPH software. In the HRTEM images, the positions of the intensity maxima at each barium and strontium atom column (bright spots in Fig. 4) were taken to measure the lattice constants. The measured lattice parameters for BTO/STO superlattices and theoretical lattice parameters for bulk BTO and STO are shown in Table 1. By comparing the lattice parameters for the bulk and superlattices in Table 1, it can be deduced that STO develops a tetragonal distortion. It has been reported that STO in the BTO/STO superlattices could have an orthorhombic distortion [10–12].

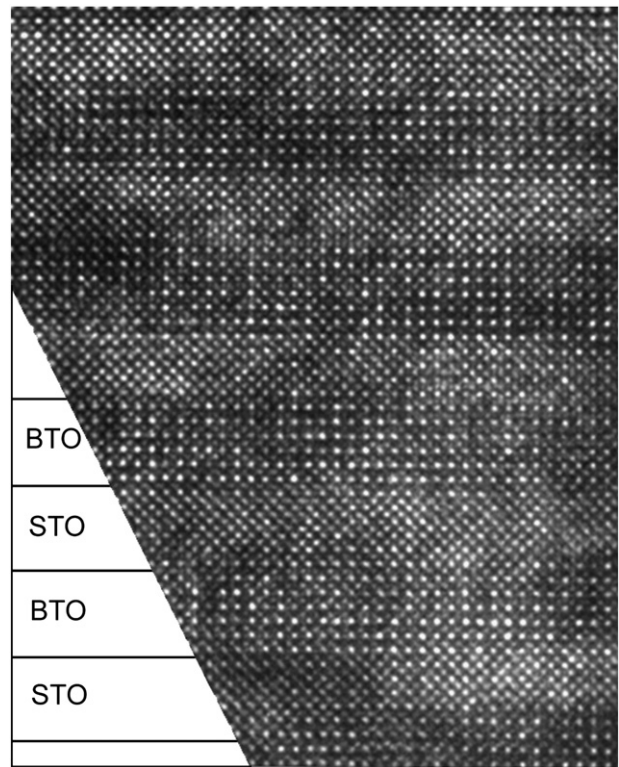


Fig. 4. Typical HRTEM image of BTO/STO superlattice showing no misfit dislocations.

From the above analyses, it can be seen that the defect states are clearly different in the single-layered and multilayered films. This is associated with the critical thickness for the formation of misfit dislocations. In order to determine the critical thicknesses for the formation of misfit dislocations in the single layered $\text{Ba}_{0.5}\text{Sr}_{0.5}\text{TiO}_3$ and BTO/STO superlattices, Matthews–Blakeslee and other critical thickness models [13–15] have been used. The critical thickness for the single-layered film is calculated to be 2.62 nm, while for the BTO/STO superlattices, the critical thickness is calculated to be 4.62 nm. The single layered $\text{Ba}_{0.5}\text{Sr}_{0.5}\text{TiO}_3$ film (1 μm is much thicker than the critical thickness, while the superlattice layer (2 nm each layer) is thinner than the critical thickness. Therefore, the lattice mismatch between LaAlO_3 substrate and $\text{Ba}_{0.5}\text{Sr}_{0.5}\text{TiO}_3$ single-layered film could only be released through the formation of misfit dislocations, while the lattice mismatch between BTO and STO superlattices can be accommodated by the lattice elastic distortion. That is why a lot of misfit dislocations are included in the single layered film, and no misfit dislocations are observed in the multilayered film. This might be one cause of the different behaviors of the permittivity with temperature in the single-layered and multilayered films.

In addition, it should be noted that STO layer in the multilayered film undergoes a tetragonal distortion. It was found that the dielectric properties of films were sensitive to the lattice distortion ratio ($D = \text{in-plane lattice constant/out-of-plane lattice constant}$), and a

Table 1
The measured lattice parameters for BTO/STO superlattices and theoretical lattice parameters for bulk BTO and STO.

Materials	Lattice parameters (Å)		
	a	b	c
BTO superlattice	3.82		4.06
BTO bulk	3.99		4.03
STO superlattice	3.82		3.98
STO bulk	3.91		3.91

film under small tensile stress showed the largest dielectric permittivity and tenability [16]. Therefore, the tetragonal distortion of STO layer could be another cause of the improved thermo-stability for the multilayered film.

4. Conclusions

In conclusion, $\text{Ba}_{0.5}\text{Sr}_{0.5}\text{TiO}_3$ single-layered and $(\text{BTO})_5/(\text{STO})_5$ multilayered epitaxial films have been grown on a (001) LaAlO_3 substrate using single target and dual target PLD, respectively. Misfit and threading dislocations have been observed in the single-layered $\text{Ba}_{0.5}\text{Sr}_{0.5}\text{TiO}_3$ film while only threading dislocations are found in the multilayered BTO/STO film. It is suspected that the difference in dislocation densities is responsible for the different behaviors of the permittivity with temperature.

Acknowledgments

The authors would like to thank the financial support from the National Natural Science Foundation of China (Grant no. 10974105), the Natural Science Foundation for Outstanding Young Scientists in Shandong Province (Grant no. JQ201002), the Project of Introducing Talents to Support Thousand Talents Programs (Grant no. P201101032), the Program of Science and Technology in Qingdao City (Grant no. 11-2-4-23-hz), and the Scientific Research Starting Foundation for the

Introduced Talents at Qingdao University (Grant no. 06300701). One author (Y.Q. Wang) would also like to thank the financial support from the Taishan Outstanding Overseas Scholar Program of Shandong Province.

References

- [1] D.E. Kotechi, *Integr. Ferroelectr.* 16 (1997) 1.
- [2] K. Bouzeshouane, P. Woodall, B. Marchilhas, A.N. Khodan, D. Crete, E. Jacquet, J.C. Mage, J.P. Contour, *Appl. Phys. Lett.* 80 (2002) 109.
- [3] N.M. Alford, *Mater. World* 15 (2007) 27.
- [4] E. Schmidgall, R.A. Walters, A. Centeno, P.K. Petrov, N.M. Alford, *Electron. Lett.* 46 (2010) 277.
- [5] K. Sarma, R. Farooq, K. Jarman, R. Pullar, P.K. Petrov, N.M. Alford, *Integr. Ferroelectr.* 62 (2004) 249.
- [6] G. Koebornik, W. Haessler, R. Pantou, F. Weiss, *Thin Solid Films* 449 (2004) 80.
- [7] T.U. Kim, B.R. Kim, W.J. Lee, J.H. Moon, B.T. Lee, J.H. Kim, *J. Cryst. Growth* 289 (2006) 540.
- [8] Y.Q. Wang, W.S. Liang, P.K. Petrov, N.M. Alford, *Mater. Charact.* 62 (2011) 294.
- [9] Y.Q. Wang, W.S. Liang, P.K. Petrov, N.M. Alford, *Appl. Phys. Lett.* 98 (2011) 091910.
- [10] W. Tian, J.C. Jiang, X.Q. Pan, J.H. Haeni, Y.L. Li, L.Q. Chen, D.G. Schlom, J.B. Neaton, K.M. Rabe, Q.X. Jia, *Appl. Phys. Lett.* 89 (2006) 092905.
- [11] S. Rios, A. Ruediger, A.Q. Jiang, J.F. Scott, H. Lu, Z. Chen, *J. Phys. Condens. Matter* 15 (21) (2003) L305.
- [12] J.B. Neaton, K.M. Rabe, *Appl. Phys. Lett.* 82 (2003) 1586.
- [13] J.W. Matthews, A.E. Blakeslee, *J. Cryst. Growth* 27 (1974) 118.
- [14] R. People, J.C. Bean, *Appl. Phys. Lett.* 47 (3) (1985) 322.
- [15] A. Braun, K.M. Briggs, P. Böni, *J. Cryst. Growth* 241 (2002) 231.
- [16] P. Bao, T.J. Jackson, X. Wang, M.J. Lancaster, *J. Phys. D: Appl. Phys.* 41 (2008) 063001.